

Photophysical Properties of Ruthenium(II) Polyazaaromatic Compounds: A Theoretical Insight

Geoffrey Pourtois,^{†,‡} David Beljonne,^{†,‡} Cécile Moucheron,[§] Stephan Schumm,^{§,||} Andrée Kirsch-De Mesmaeker,[§] Roberto Lazzaroni,^{†,‡} and Jean-Luc Brédas^{*,†,‡}

Contribution from the Laboratory for Chemistry of Novel Materials, University of Mons-Hainaut, 20 Place du Parc, B-7000 Mons, Belgium, Department of Chemistry, The University of Arizona, Tucson, Arizona 85721-0041, Laboratory of Organic Chemistry and Photochemistry, CP 160/08, Université Libre de Bruxelles, 50 Av. F.D. Roosevelt, B-1050 Bruxelles, Belgium, and Unilever R&D Colworth, Colworth House Sharnbrook, Bedford MK40 1LQ, United Kingdom

Received January 31, 2003; E-mail: jean-luc.bredas@chemistry.gatech.edu

Abstract: Quantum-chemical methods are applied to study the nature of the excited states relevant in the photophysical processes (absorption and emission) of a series of polyazaaromatic-ligand-based ruthenium(II) complexes. The electronic and optical properties of the free polyazaaromatic ligands and their corresponding ruthenium(II) complexes are determined on the basis of correlated Hartree–Fock semiempirical approaches. While the emission of complexes containing small-size ligands, such as 1,10-phenanthroline or 2,2'-bipyridine, arises from a manifold of metal-to-ligand charge-transfer triplet states (³MLCTs), an additional ligand-centered triplet state (³L) is identified in the triplet manifold of complexes containing a π -extended ligand such as dipyrido[3,2-*a*:2',3'-*c*]phenazine, tetrapyrido[3,2-*a*:2',3'-*c*:3'',2''-*h*:2''',3'''-*j*]phenazine, and 1,10-phenanthroline[5,6-*b*]-1,4,5,8,9,12-hexaazatriphenylene. Recent experimental data are interpreted in light of these theoretical results; namely, the origin for the abnormal solvent- and temperature-dependent emission measured in π -extended Ru complexes is revisited.

I. Introduction

Molecular architectures based on the assembly of metallic cores and aromatic ligands are currently among the most studied compounds in coordination chemistry because of their unique combination of chemical stability, excited-state reactivity, and redox properties responsible for specific electron- and energy-transfer processes.^{1,2} The stakes not only are fundamental but have important implications in the development of numerous applications, such as organic light-emitting diodes,³ photoelectrochemical cells,^{4–7} biological and medical diagnostics⁸ tools, and development of therapeutic agents.^{9–12} For instance,

platinum complexes have been widely used in cancer chemotherapy since the late 1970s.^{13,14} Among these complexes, cisplatin(II) and derivatives have shown significant activity against various types of tumors,¹⁵ but their severe toxicity has motivated research for new candidates, such as complexes based on Ru(II), Ru(III), or Os(II) ions.

Recent developments have shown that Ru(II) complexes can inhibit DNA transcription.¹⁶ It has been demonstrated that these complexes easily bind to DNA and cleave it or form adducts upon photoexcitation.^{17–19} These properties are promising for the design of DNA markers and agents in photochemotherapy. One major challenge in the development of such applications is the need to control and characterize the photophysical properties of these metallic complexes, as a function of the nature of the core ion and the ligand(s).^{2,20} These positively charged Ru(II) compounds have an octahedral configuration, and their photochemical and photophysical properties can be

* To whom correspondence should be addressed.

[†] University of Mons-Hainaut.

[‡] The University of Arizona.

[§] Université Libre de Bruxelles.

^{||} Unilever R&D Colworth.

- (1) Balzani, V.; Juris, A.; Venturi, M. *Chem. Rev.* **1996**, *96*, 759.
- (2) Ortmans, I.; Moucheron, C.; Kirsch-de Mesmaeker, A. *Coord. Chem. Rev.* **1997**, *168*, 233.
- (3) Gao, F. G.; Bard, A. J. *J. Am. Chem. Soc.* **2000**, *122*, 7426–7427.
- (4) Meyer, G. J. *J. Chem. Educ.* **1997**, *74*, 652.
- (5) Hagfeldt, A.; Grätzel, M. *Chem. Rev.* **1995**, *95*, 49.
- (6) Heimer, T. A.; Bignozzi, C. A.; Meyer, G. J. *J. Phys. Chem.* **1993**, *97*, 11987.
- (7) Hennig, H.; Billing, R.; Knoll, H. *Photosensitisation and Photocatalysis Using Inorganic and Organometallic Compounds*; Kluwer Academic Publishers: Dordrecht, The Netherlands, 1993.
- (8) Armistead, P. M.; Thorp, H. H. *Bioconjugate Chem.* **2002**, *13*, 172.
- (9) Kirsch-De Mesmaeker, A.; Lecomte, J. P.; Kelly, J. M. *Top. Curr. Chem.* **1996**, *177*, 25.
- (10) Klimant, I.; Wolfbeiss, O. S. *Anal. Chem.* **1995**, *34*, 3160.
- (11) Erkkila, K. E.; Odom, D. T.; Barton, J. K. *Chem. Rev.* **1999**, *99*, 2777.
- (12) Barton, J. K. *Science* **1986**, *233*, 727.

- (13) Bruhn, S.; Toney, J.; Lippard, S. J. *Prog. Inorg. Chem. Bioinorg. Chem.* **1990**, *38*, 477–516.
- (14) Sundquist, W. I.; Lippard, S. J. *Coord. Chem. Rev.* **1990**, *100*, 293–322.
- (15) Lippard, S. J.; Berg, J. M. *Principles of Bioinorganic Chemistry*; University Science Books: Mill Valley, CA, 1994.
- (16) Pauly, M.; Kayser, I.; Schmitz, M.; Dicato, M.; Del Guerso, A.; Kolber, I.; Moucheron, C.; Kirsch-De Mesmaeker, A. *Chem. Commun.* **2002**, 1986.
- (17) Jacquet, L.; Davies, R. J. H.; Kirsch-De Mesmaeker, A.; Kelly, J. M. *J. Am. Chem. Soc.* **1997**, *119*, 11763.
- (18) Lecomte, J. P.; Kirsch-De Mesmaeker, A.; Feeney, M.; Kelly, J. M. *Inorg. Chem.* **1995**, *34*, 6481.
- (19) Friedman, A. E.; Chambron, J. C.; Sauvage, J. P.; Turro, N. J.; Barton, J. K. *Nucleic Acids Res.* **1984**, *13*, 6016–6034.
- (20) Moucheron, C.; Kirsch-De Mesmaeker, A.; Kelly, J. M. *J. Photochem. Photobiol., B* **1997**, *40*, 91.

modulated by the type of ligands. For instance, the substitution of one (or several) ligand(s) in $[\text{Ru}(\text{bpy})_3]^{2+}$ (bpy = 2,2'-bipyridine) or $[\text{Ru}(\text{phen})_3]^{2+}$ (phen = 1,10-phenanthroline) by a ligand containing additional unchelated nitrogen atoms in the aromatic rings (such as 1,4,5,8-tetraazaphenanthrene (tap) or 1,4,5,8,9,12-hexaazatriphenylene (hat)) makes the resulting complex more photooxidizing.^{2,18,20,21}

In the case of these complexes containing two or three of these oxidizing ligands, it has been shown that the emission is quenched by the DNA nucleobases through an electron-transfer process, which leads to DNA damage such as strand cleavage or formation of adducts of the complexes on DNA bases.^{21,22} On the other hand, the substitution of one ligand in $[\text{Ru}(\text{bpy}/\text{phen})_3]^{2+}$ by dipyrido[3,2-*a*:2',3'-*c*]phenazine (dppz),^{23–26} tetrapyrido[3,2-*a*:2',3'-*c*:3'',2''-*h*:2''',3'''-*j*]phenazine (tpphz),²⁷ or 1,10-phenanthroline[5,6-*b*]-1,4,5,8,9,12-hexaazatriphenylene (phehat)^{28,29} leads to a complex which does not luminesce in water but whose emission is switched on by interaction with DNA. The quenching of luminescence in water has been attributed to the presence of a low-lying Ru–dppz metal-to-ligand charge-transfer triplet excited state stabilized by the formation of hydrogen bonds.^{30,31} More recent experimental data suggest that even in aprotic solvents the rationalization of the temperature-dependent emission lifetime requires accounting for different decay channels, which once again underlines the complex photophysical properties of these compounds.³²

To shed light on these processes, we study in this paper the influence of the chemical nature of the ligand on the photophysical properties of a set of ruthenium(II) polyazaaromatic molecules: $[\text{Ru}(\text{phen})_3]^{2+}$, $[\text{Ru}(\text{dppz})(\text{phen})_2]^{2+}$, $[\text{Ru}(\text{tpphz})(\text{phen})_2]^{2+}$, and $[\text{Ru}(\text{phehat})(\text{phen})_2]^{2+}$ (Figure 1).

Several experimental and theoretical studies have been devoted to the examination of the effects of different polyazaaromatic ligands on the complex properties.^{33–38} Quantum-chemical investigations have been based on either semiempirical approaches^{33,36–41} or density functional theory (DFT)^{34,42–45}

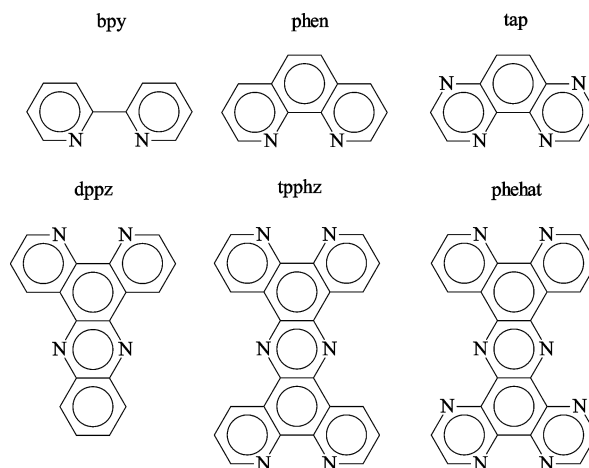


Figure 1. Structures of the polyazaaromatic ligands considered in this work.

(when applied to second-row transition metals, the ab initio Hartree–Fock formalism suffers from the relatively large atomic size, in terms of atomic orbital basis set and the lack of electron correlation, which is known to play an important role in the description of the geometric and electronic structure of coordination complexes⁴⁶). As an alternative to ab initio calculations, semiempirical methods are widely exploited; among the most popular semiempirical methods, CNDO,⁴⁷ MNDO-d,^{48–50} and intermediate neglect of differential overlap (INDO)-based methods^{51,52} can handle transition-metal atoms. Here, we have chosen to use the INDO formalism, which we have previously exploited with success to investigate the excited-state characteristics of porphyrin-based complexes;⁵³ time-dependent density functional theory (TDDFT) calculations were also performed to check the particular excited-state ordering predicted in $[\text{Ru}(\text{dppz})(\text{phen})_2]^{2+}$ at the INDO level, vide infra.

We first focus on the electronic and optical properties of the free polyazaaromatic ligands; we mainly consider the influence of the extension of the aromatic backbone on the electronic structure in the ground state and in the lowest singlet and triplet excited states. We then describe the electronic properties of the corresponding complexes and discuss the nature of the electronic transitions occurring upon photoexcitation. Finally, the energies and the spatial distribution of the triplet excited state wave functions are analyzed in relation to the mechanism of emission of these complexes.

II. Theoretical Methodology

The ground-state geometry of all free ligands was first fully optimized at the semiempirical Hartree–Fock level of theory using the Austin model 1 (AM1) method, which is known to provide reliable ground-state and excited-state geometric structures for conjugated

- (21) Moucheron, C.; Kirsch-De Mesmaeker, A.; Kelly, J. M. *Structure and Bonding*; Boston College: Boston, MA, 1998; Vol. 92.
- (22) Lecomte, J. P.; Kirsch-De Mesmaeker, A.; Kelly, J. M.; Tossi, A.; Gömer, H. *Photochem. Photobiol.* **1992**, *55*, 681.
- (23) Friedman, A. E.; Chambron, J. C.; Sauvage, J. P.; Turro, N. J.; Barton, J. K. *J. Am. Chem. Soc.* **1990**, *112*, 4960.
- (24) Lincoln, P.; Broo, A.; Nordén, B. *J. Am. Chem. Soc.* **1996**, *118*, 2644–2653.
- (25) Hört, C.; Lincoln, P.; Nordén, B. *J. Am. Chem. Soc.* **1993**, *115*, 3448.
- (26) Ujj, L.; Coates, C. G.; Kelly, J. M.; Krüger, P. E.; McGarvey, J. J.; Atkinson, G. H. *J. Phys. Chem. B* **2002**, *106*, 4854.
- (27) Bolger, J.; Gourdon, A.; Ishow, E.; Launay, J. P. *Inorg. Chem.* **1996**, *35*, 2937.
- (28) Moucheron, C.; Kirsch-De Mesmaeker, A.; Choua, S. *Inorg. Chem.* **1997**, *36*, 584.
- (29) Moucheron, C.; Kirsch-De Mesmaeker, A. *J. Phys. Org. Chem.* **1998**, *577*.
- (30) Olson, E. J. C.; Hu, D.; Hormann, A.; Jonkman, A. M.; Arkin, M. R.; Stemp, E. D. A.; Barton, J. K.; Barbara, P. F. *J. Am. Chem. Soc.* **1997**, *119*, 11458–11467.
- (31) Önfelt, B.; Olofsson, J.; Lincoln, P.; Nordén, B. *J. Phys. Chem. A* **2003**, *107*, 1000.
- (32) Brenneman, M. K.; Alstrum-Acevedo, J. H.; Fleming, C. N.; Jang, P.; Meyer, T. J.; Papanikolas, J. M. *J. Am. Chem. Soc.* **2002**, *124*, 15094.
- (33) Broo, A.; Lincoln, P. *Inorg. Chem.* **1997**, *36*, 2544.
- (34) Daul, C.; Baerends, E.; Vernooijs, P. *Inorg. Chem.* **1994**, *33*, 3538–3543.
- (35) Larsson, S.; Broo, A.; Källebring, B.; Volosov, A. *Int. J. Quantum Chem., Quantum Biol. Symp.* **1988**, *16*, 185.
- (36) Reimers, J. R.; Hush, N. S. *J. Chem. Phys.* **1991**, *95*, 9773.
- (37) Zeng, J.; Hush, N. S.; Reimers, J. R. *J. Chem. Phys.* **1995**, *99*, 10459.
- (38) Stavrev, K. K.; Zerner, M. C.; Meyer, T. J. *J. Am. Chem. Soc.* **1995**, *117*, 8684.
- (39) Broo, A.; Larsson, S. *Chem. Phys.* **1992**, *161*, 363.
- (40) Yutaka, T.; Mori, I.; Kurihara, M.; Mizutani, J.; Kubo, K.; Furusho, S.; Matsumura, K.; Tamai, N.; Nishihara, H. *Inorg. Chem.* **2001**, *40*, 4986.
- (41) Gorelsky, S. I.; Dodsworth, E. S.; Lever, A. B. P.; Vlcek, A. A. *Coord. Chem. Rev.* **1998**, *174*, 469.

- (42) Zhang, L. T.; Ko, J.; Ondrechen, M. J. *J. Am. Chem. Soc.* **1987**, *109*, 1666.
- (43) Albano, G.; Belsler, P.; Daul, C. *Inorg. Chem.* **2001**, *40*, 1408.
- (44) Stoyanov, S. R.; Villegas, J. M.; Rillema, D. P. *Inorg. Chem.* **2002**, *41*, 2941.
- (45) Monat, J. E.; Rodriguez, J. H.; McCusker, J. J. *Phys. Chem. A* **2002**, *106*, 7399.
- (46) Siegbahn, P. E. M.; Svensson, M. *Chem. Phys. Lett.* **1993**, *216*, 147.
- (47) Pople, J. A.; Santry, D. P.; Segal, G. A. *J. Chem. Phys.* **1965**, *43*, 129.
- (48) Thiel, W.; Voityuk, A. A. *THEOCHEM* **1994**, *313*, 141.
- (49) Thiel, W.; Voityuk, A. A. *J. Phys. Chem.* **1996**, *100*, 616.
- (50) Thiel, W. *Adv. Chem. Phys.* **1996**, *93*, 703.
- (51) Jug, K.; Nanda, D. N. *Theor. Chim. Acta* **1980**, *57*, 95.
- (52) Ridley, J.; Zerner, M. C. *Theor. Chim. Acta* **1973**, *32*, 111.
- (53) Beljonne, D.; Wittmann, H. F.; Kohler, A.; Graham, S.; Younus, M.; Lewis, J.; Raitzhe, P. R.; Khan, M. S.; Friend, R. H.; Brédas, J. L. *J. Chem. Phys.* **1996**, *105*, 3868.

organic molecules.^{54–56} In the absence of ruthenium parametrization in AM1, the ground-state geometries of the corresponding complexes were then built on the basis of the free ligands and optimized via the semiempirical Hartree–Fock INDO Hamiltonian implemented in the ZINDO package.⁵² We adopted the ruthenium(II) ion parametrization proposed by Broo et al.³³ and imposed the $4d^65s^0$ electronic configuration for the geometry optimization. The optimized geometries display the highest accessible degree of symmetry and are in very good agreement with crystallographic data.³³

The equilibrium geometries in the triplet excited states of the free ligands were obtained by combining the AM1 approach with a complete active space configuration interaction (AM1/CAS-CI) treatment (as developed in the AMPAC package⁵⁷). The size of the active space in the AM1/CAS-CI calculations was modulated to ensure convergence of the heat of formation and geometric parameters. The number of occupied and unoccupied molecular orbitals involved in the active space typically varies from 10 to 20 along the series of the examined ligands.

The INDO Hamiltonian was then combined with a single configuration interaction (SCI) scheme to describe the singlet and triplet excited states. The singlet- and triplet-excited-state energies were computed with the electron–electron repulsion potentials developed by Ohno and Klopman^{58,59} (except for the description of the singlet excited states in the inorganic compounds, where the Mataga–Nishimoto⁶⁰ potential, which was originally adopted to parametrize the INDO method against singlet absorption spectra, was used). The size of the CI active space was modulated to ensure convergence of the calculated transition energies. In contrast to the approach adopted for geometry optimization,³³ we did not impose in this case the $4d^65s^0$ electronic configuration on the ruthenium(II) center when computing the excited states but rather used a valence bond mixing among the $4d^45s^2$, $4d^55s^1$, and $4d^65s^0$ configurations. Indeed, we found that allowing a larger flexibility to the ruthenium(II) electronic configuration leads to a better agreement (by about 0.2 eV) between the calculated and measured absorption energies. A zero differential overlap (ZDO) population analysis was performed to analyze the characteristics of the excited states; the localization of the triplet excitations was evaluated on the basis of the spin density distribution, defined as the difference between the α and β electron spin densities. The absorption spectra were simulated via the INDO excitation energies and oscillator strengths considering Gaussian line shapes with a 0.2 eV width at half-maximum. Solvent effects were estimated in an implicit way by using a self-consistent reaction field (SCRF) treatment based on Onsager theory (considering ellipsoidal cavities).⁶¹

The Franck–Condon gas-phase triplet-excited-state energies were determined by an INDO/SCI and (in the case of the $[\text{Ru}(\text{dppz})(\text{phen})_2]^{2+}$ complex) a time-dependent DFT treatment^{62–65} on the ground-state geometry of the complexes (optimized at the INDO and DFT levels, respectively). The TDDFT calculations were performed at the DFT-optimized ground-state geometry using the Gaussian 98 program and the MPW1PW91⁶⁶ hybrid functional to account for the exchange–correlation potential. The chosen basis sets are 6-31G* for the carbon, nitrogen, and hydrogen atoms and an SDD (Stuttgart/Dresden)^{67,68}

pseudopotential on the ruthenium core. An unpruned Lebedev grid of 75 radial and 302 angular points was employed in all DFT calculations.

Modeling the geometric relaxations taking place in the triplet excited states of coordination complexes is a formidable task. Methodologies based on correlated ab initio techniques (such as CASSCF^{69–72}) rapidly become computationally intractable for systems as large as $[\text{Ru}(\text{bpy})_3]^{2+}$. In addition, to the best of our knowledge, there is no reliable semiempirical quantum-chemical method allowing this problem to be tackled. Here, we used a very simple approach to gain some insight into the influence of the effects of geometric relaxation on the energies of the triplet excited states in the Ru complexes investigated. The geometric relaxations of those complexes were modeled in the following way: we first optimized the free ligand geometry in the lowest triplet state at the AM1/CAS-CI level of theory; we then incorporated this geometry into the ground-state structure of the complex, keeping the ruthenium–ligand bond lengths and angles constant. In symmetric complexes such as $[\text{Ru}(\text{bpy})_3]^{2+}$ or $[\text{Ru}(\text{phen})_3]^{2+}$, the mechanism for the relaxation dynamics in the excited state is rather controversial.^{73–76} There are two possible scenarios, depending on the relative magnitude of the geometric relaxation energy (E^{rel}) in a free ligand and the electronic coupling (V) among the ligands: (i) If $V > E^{\text{rel}}$, the excitation remains delocalized over the three ligands; in that case, the lowest triplet states remain degenerate and are likely to participate equally in the emission process.^{77–81} We considered a very simple model, where it is assumed that the overall geometric modifications can be evenly distributed among the three ligands. In the 3-fold symmetric molecules investigated, the geometry distortion in each ligand was therefore set at one-third its magnitude in the free ligand. (ii) If $V < E^{\text{rel}}$, it is energetically favorable to localize the deformations on a single ligand; the degeneracy of the excited states is lifted together with a reduction in molecular symmetry from D_3 to C_2 .⁷⁵ We then proceeded as in the case of an asymmetric substitution. We note that the interactions between the excited species and the environment are key factors in the dynamics of excitation localization; e.g., the solvent moment of inertia has been shown to be strongly correlated to the excitation localization mechanism.⁷⁵

III. Electronic Structure of the Isolated Ligands

The optical properties of the ruthenium(II) complexes are primarily related to the nature of the polyazaaromatic ligands. In the bpy, phen, dppz, tpphz, and phehat sequence, the electronic structure (Figure 2) is governed by two main factors: (i) the size of the conjugated backbone (the more extended the conjugation, the smaller the HOMO–LUMO gap), and (ii) the chemical nature of the ligand (substitution of CH units by nitrogen atoms in the aromatic rings leads to a stabilization of both frontier electronic levels; e.g., in going from

- (54) Cornil, J.; Beljonne, D.; Brédas, J. L. *J. Chem. Phys.* **1995**, *103*, 843.
 (55) Almlöf, J.; Fischer, T. H.; Gassman, P. G.; Ghosh, A.; Häser, M. *J. Phys. Chem.* **1993**, *97*, 10964.
 (56) Merchan, M.; Orti, E.; Roos, B. O. *Chem. Phys. Lett.* **1994**, *226*, 27.
 (57) Dewar, M. J. S. Ampac 6.55, Semicem, 7204 Mullen, Shawnee, KS 66216, 1997.
 (58) Ohno, K. *Theor. Chim. Acta* **1964**, *2*, 219.
 (59) Klopman, G. *J. Am. Chem. Soc.* **1964**, *86*, 4550.
 (60) Mataga, N.; Nishimoto, K. *Z. Phys. Chem.* **1957**, *13*, 140.
 (61) Karelson, M. M.; Zerner, M. C. *J. Phys. Chem.* **1992**, *96*, 6949–6957.
 (62) Jamorski, C.; Foresman, J. B.; Thilgen, C.; Luthi, H. P. *J. Chem. Phys.* **2002**, *116*, 8761.
 (63) Lodicke, C. J.; Luthi, H. P. *J. Chem. Phys.* **2002**, *117*, 4146.
 (64) Cavillot, V.; Champagne, B. *Chem. Phys. Lett.* **2002**, *354*, 449.
 (65) Ghizdavu, L.; Lentzen, O.; Schumm, S.; Brodtkorb, A.; Moucheron, C.; Kirsch-DeMesmaecker, A. *Inorg. Chem.* **2003**, *42*, 1935.
 (66) Adamo, C.; Barone, V. *J. Chem. Phys.* **1998**, *108*, 664.
 (67) Dolg, M.; Stoll, H.; Preuss, H. *Theor. Chim. Acta* **1993**, *85*, 441.

- (68) Wedig, U.; Dolg, M.; Stoll, H. *Quantum Chemistry: The Challenge of Transition Metals and Coordination Chemistry*; Dordrecht, The Netherlands, 1986.
 (69) Eade, R. H. E.; Robb, M. A. *Chem. Phys. Lett.* **1981**, *83*, 362.
 (70) Hegarty, D.; Robb, M. A. *Mol. Phys.* **1979**, *38*, 1795.
 (71) Roos, B. O.; Taylor, P. R. *Chem. Phys.* **1980**, *48*, 157.
 (72) Siegbahn, P. E. M.; Almlöf, J.; Heiberg, A.; Roos, B. O. *J. Chem. Phys.* **1981**, *74*.
 (73) Bradley, P. G.; Kress, N.; Hornberger, B. A.; Dallinger, R. F.; Woodruff, W. H. *J. Am. Chem. Soc.* **1981**, *103*, 7441.
 (74) Turro, C.; Chung, Y. C.; Leventis, N.; Kuchenmeister, M. E.; Wagner, P. J.; Leroi, G. E. *Inorg. Chem.* **1996**, *33*, 5104.
 (75) Yeh, A. T.; Shank, C. V.; McCusker, J. K. *Science* **2000**, *289*, 935–938.
 (76) Schoonover, J. R.; Omberg, K. M.; Moss, J. A.; Bernhard, S.; Malueg, V. J.; Woodruff, W. H.; Meyer, T. J. *Inorg. Chem.* **1998**, *37*, 2585.
 (77) Juris, A.; Balzani, V.; Barigelli, F.; Campagna, S.; Belser, P.; Von Zelewsky, A. *Coord. Chem. Rev.* **1988**, *84*, 85–277.
 (78) Lumpkin, R. S.; Kober, E. M.; Worl, L. A.; Murtaza, Z.; Meyer, T. J. *J. Phys. Chem.* **1990**, *94*, 239–243.
 (79) Kirk, A. D.; Hoggard, P. E.; Porter, G. B.; Rockley, M. G.; Windsor, M. W. *Chem. Phys. Lett.* **1976**, *37*, 199–203.
 (80) Maruszewski, K.; Bajdor, K.; Strommen, D. P.; Kincaid, J. R. *J. Phys. Chem.* **1995**, *99*, 6286–6293.
 (81) Meyer, T. J. *Pure Appl. Chem.* **1986**, *58*, 1193–1206.

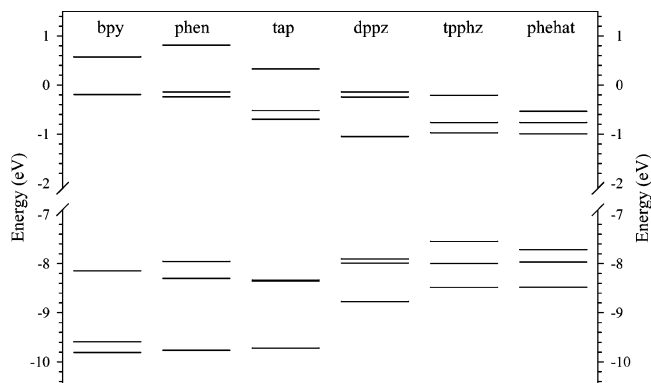


Figure 2. Evolution of the INDO energies of the three highest occupied and the three lowest unoccupied molecular orbitals in the free ligands.

Table 1. Lowest Triplet-Excited-State (E_{T_1} and E_{T_2}) and Singlet-Excited-State (E_{S_1}) Energies Computed at the INDO/SCI Level for Bpy, Phen, Tap, Dppz, Tpphz, and Phehat (eV)^a

	E_{T_1}	E_{T_2}	E_{S_1}	K_{eff}
bpy	2.68	3.25	4.28	-1.60
phen	2.45	3.25	4.70	-2.25
tap	2.42	2.86	4.23	-1.81
dppz	2.32	2.42	3.58	-1.26
tpphz	2.27	2.31	3.31	-1.04
phehat	2.27	2.42	3.45	-1.18

^a The effective exchange energy (K_{eff}) is computed as $K_{\text{eff}} = (E_{T_1} - E_{S_1})$. The singlet- and triplet-excited-state energies are evaluated with the repulsion potential developed by Ohno⁵⁸ and Klopman.⁵⁹

phen to tap, the HOMO and LUMO levels are both stabilized by about 0.4 eV; see Figure 2).

For all the ligands, the HOMO shows the same bonding–antibonding pattern; it is delocalized over the whole ligand with relatively small LCAO (linear combination of atomic orbitals) coefficients on the nitrogen atoms, especially on the central pyrazine core of dppz, tpphz, and phehat. Due to the inductive effect of the nitrogens, the energy of the HOMO gets stabilized from phen to tap. It is then progressively destabilized in the sequence $\text{tap} < \text{dppz} < \text{tpphz}$ as a consequence of increased π -delocalization. Compared to that of tpphz, the HOMO level of phehat is stabilized owing to the presence of two more nitrogen atoms.

The LUMO also shows common characteristics in the whole series: it is delocalized over the ligand with a larger contribution on the nitrogens for phen and tap. Similarly to that of the HOMO, the stabilization of the LUMO, on going from phen to tap, stems from the inductive effect of the nitrogen atoms. In dppz, tpphz, and phehat, the LUMOs are quasi-isoenergetic and share a common origin: their wave functions are mainly localized on the inner part of the molecules with dominant contributions on the nitrogen atoms of the central pyrazine unit. Note that the electronic structure of the tap ligand is discussed here for the sake of comparison; ruthenium(II) complexes based on tap have not been investigated in this work.

Over the series, the first optical transition (S_1) corresponds mainly to a HOMO \rightarrow LUMO excitation. It evolves as the HOMO–LUMO gap and therefore reflects the changes in electronic structure described above (see Table 1). The lowest triplet-state energy (E_{T_1}) is also sensitive to the polyazaaromatic structure.

E_{T_1} and the relative amplitude of the effective exchange energy (K_{eff}), $K_{\text{eff}} = (E_{T_1} - E_{S_1})$, evolve as E_{S_1} , i.e., parallel to

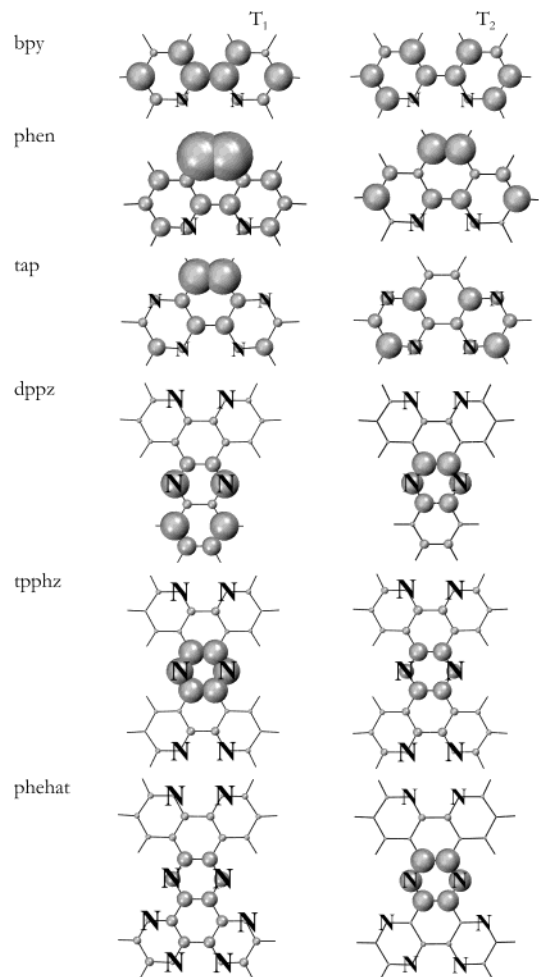


Figure 3. Spin density distribution calculated at the INDO/SCI level for the two lowest lying excited triplet states (T_1 and T_2) of the free ligands.

the HOMO–LUMO gap. The exchange stabilization energy reflects the confinement of the triplet wave function: the more localized the triplet, the larger the exchange energy. K_{eff} is found to be smaller for dppz, tpphz, and phehat than for bpy, phen, and tap (Table 1): for instance, K_{eff} amounts to -1.60 eV in bpy and -1.26 eV in dppz. Analysis of the triplet spin density, i.e., the triplet wave function, indicates (Figure 3) that the spin density is pretty much delocalized over the whole ligands (with some more “local” contributions for dppz, tpphz, and phehat); K_{eff} is therefore calculated to be smaller in the extended ligands.

IV. Photophysical Properties of the Ruthenium(II) Complexes

In its +2 oxidation state, the ruthenium atom adopts a low-spin $4d^65s^0$ electronic configuration, in which three d orbitals are doubly occupied and two are empty. For the complexes investigated, the ligand field around the central ruthenium ion shows a quasi-octahedral symmetry (O_h). In the case of a perfect O_h ligand field, the occupied and unoccupied orbitals are degenerate and have either t_{2g} or e_g symmetry.

IV.1. Absorption Properties. In the series $[\text{Ru}(\text{phen})_3]^{2+}$, $[\text{Ru}(\text{dppz})(\text{phen})_2]^{2+}$, $[\text{Ru}(\text{tpphz})(\text{phen})_2]^{2+}$, and $[\text{Ru}(\text{phehat})(\text{phen})_2]^{2+}$, the lowest lying unoccupied levels are localized on the most “ π -extended” ligand. Therefore, their energies qualitatively follow the same sequence as that calculated for the empty levels on the ligands. The three highest occupied

Table 2. Optically Allowed Electronic Transitions in $[\text{Ru}(\text{phen})_3]^{2+}$ and $[\text{Ru}(\text{dppz})(\text{phen})_2]^{2+}$ Calculated at the INDO/SCI Level^a

$[\text{Ru}(\text{phen})_3]^{2+}$				$[\text{Ru}(\text{dppz})(\text{phen})_2]^{2+}$			
<i>E</i> (eV)	OS	assignment		<i>E</i> (eV)	OS	assignment	
3.08 [2.79]	0.13	$\text{Ru} \rightarrow \pi^*_{\text{phen}}$	1	2.92 [2.82]	0.35	$\text{Ru} \rightarrow \pi^*_{\text{dppz}}$	1
3.08	0.12	$\text{Ru} \rightarrow \pi^*_{\text{phen}}$		3.14 [3.37]	0.15	$\text{Ru} \rightarrow \pi^*_{\text{phen}}$	
3.55 [3.00]	0.18	$\text{Ru} \rightarrow \pi^*_{\text{phen}}$	2	3.39 [3.44]	0.16	$\pi_{\text{dppz}} \rightarrow \pi^*_{\text{dppz}}$	
3.55	0.18	$\text{Ru} \rightarrow \pi^*_{\text{phen}}$		3.62	0.17	$\text{Ru} \rightarrow \pi^*_{\text{phen}}$	2
4.33 [3.95]	0.15	$\pi_{\text{phen}} \rightarrow \pi^*_{\text{phen}}$	3	3.65 [3.52]	0.42	$\text{Ru} \rightarrow \pi^*_{\text{dppz}}$	
4.33	0.15	$\pi_{\text{phen}} \rightarrow \pi^*_{\text{phen}}$		3.95 [3.92]	0.10	$\text{Ru} \rightarrow \pi^*_{\text{phen}}$	
4.36	0.32	$\pi_{\text{phen}} \rightarrow \pi^*_{\text{phen}}$		4.13	0.13	$\text{Ru} \rightarrow \pi^*_{\text{dppz}}$	3
4.73	0.28	$\text{Ru} \rightarrow \pi^*_{\text{phen}} + \pi_{\text{phen}} \rightarrow \pi^*_{\text{phen}}$	4	4.22	0.21	$\text{Ru} \rightarrow (\pi^*_{\text{dppz}} + \pi^*_{\text{phen}})$	
4.86	0.48	$\text{Ru} \rightarrow \pi^*_{\text{phen}} + \pi_{\text{phen}} \rightarrow \pi^*_{\text{phen}}$		4.26 [4.49]	1.20	$\pi_{\text{dppz}} \rightarrow \pi^*_{\text{dppz}}$	
4.93	1.42	$\text{Ru} \rightarrow \pi^*_{\text{phen}} + \pi_{\text{phen}} \rightarrow \pi^*_{\text{phen}}$		4.28	0.20	$\pi_{\text{dppz}} \rightarrow \pi^*_{\text{dppz}} + \text{Ru} \rightarrow \pi^*_{\text{phen}}$	
				4.38	0.58	$\pi_{\text{phen}} \rightarrow \pi^*_{\text{phen}}$	
				4.40	0.17	$\pi_{\text{phen}} \rightarrow \pi^*_{\text{phen}}$	
				4.79	0.27	$\text{Ru} \rightarrow \pi^*_{\text{phen}} + \pi_{\text{phen}} \rightarrow \pi^*_{\text{phen}}$	4
				4.90 [4.70]	1.02	$\text{Ru} \rightarrow \pi^*_{\text{phen}} + \pi_{\text{phen}} \rightarrow \pi^*_{\text{phen}}$	
				4.99	0.19	$\text{Ru} \rightarrow \pi^*_{\text{phen}} + \pi_{\text{phen}} \rightarrow \pi^*_{\text{phen}}$	

^a Only those excited states with calculated oscillator strengths ≥ 0.1 are included. *E* is the vertical transition energy and OS the associated oscillator strength. Experimental absorption maxima in acetonitrile are indicated within brackets.^{28,29,88}

molecular orbitals of the complexes reflect the combined effects of the three ligands; they are described by a combination of Ru d orbitals, phen, and π -extended contributions (mainly the “phen section” of the extended ligand that is in direct contact with the ruthenium ion).

The optically active excited states in coordination complexes are traditionally classified into five categories: charge-transfer excited states involving (i) a metal-to-ligand (MLCT), (ii) a ligand-to-ligand (LLCT), or (iii) a ligand-to-metal (LMCT) charge-transfer excitation, and localized (Frenkel-like) excitations over either (iv) a ligand (L) or (v) a metal center (M). This is, of course, a simplified picture, and we have found instances where a strong mixing between charge-transfer and localized $\pi \rightarrow \pi^*$ excitations does occur (Table 2).

In $[\text{Ru}(\text{phen})_3]^{2+}$, the lowest two optical transitions (labeled “1” and “2” in Figure 4) are predicted [measured]⁸⁴ at 3.08 [2.79] and 3.55 [3.00] eV and present an MLCT character. $\pi \rightarrow \pi^*$ (labeled “3”) and mixed $\pi \rightarrow \pi^*/\text{MLCT}$ (labeled “4”) excitations take place at higher energies, ~ 4.3 [3.95] and 4.9 eV, respectively (a similar mixed character has been observed from TDDFT calculations for cyclometalated Ir(III)⁸² and Rh(III) complexes⁸³). The presence of π -extended ligands of increasing size has a direct incidence on the absorption spectra of the Ru(II) complexes (Figure 4 and Table 2) as illustrated by the comparison between the $[\text{Ru}(\text{phen})_3]^{2+}$ and $[\text{Ru}(\text{dppz})(\text{phen})_2]^{2+}$ calculated absorption spectra:³³ substitution of a phen by a dppz ligand leads to the emergence of new MLCT and $\pi \rightarrow \pi^*$ electronic transitions involving dppz, a finding that is fully consistent with experiment (Table 2). The absorption spectrum of $[\text{Ru}(\text{dppz})(\text{phen})_2]^{2+}$ displays MLCT transitions (at energies up to 4.22 eV, Table 2) that involve essentially dppz or both phen and dppz. The population analysis indicates that the charge transferred to the dppz unit is localized on the phen section of the dppz ligand in direct contact with Ru. Calculated [measured]⁸⁴ optical signatures of the intraligand $\pi \rightarrow \pi^*$ excitation related to dppz and phen consist mainly in the absorption bands at 4.26 eV [4.49 eV] (3) and 4.90 eV [4.70 eV] (4), respectively. Interestingly, the INDO/SCI calculations

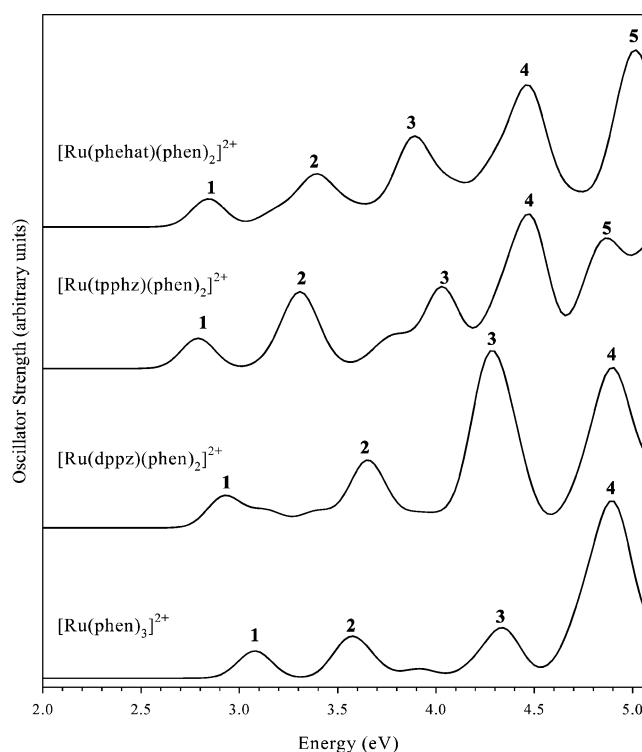


Figure 4. INDO/SCI absorption spectra of $[\text{Ru}(\text{phen})_3]^{2+}$, $[\text{Ru}(\text{dppz})(\text{phen})_2]^{2+}$, $[\text{Ru}(\text{tpphz})(\text{phen})_2]^{2+}$, and $[\text{Ru}(\text{phehat})(\text{phen})_2]^{2+}$.

indicate the presence, in dppz (as well as in the other extended ligands), of a low-lying ligand $\pi \rightarrow \pi^*$ excitation at 3.39 eV [measured at ~ 3.44 eV], i.e., slightly above the lowest MLCT singlet transitions (while the lowest $\pi \rightarrow \pi^*_{\text{phen}}$ excitation occurs at much higher energy). As described in the next section, the corresponding dppz $\pi \rightarrow \pi^*$ triplet excitation plays a major role in the mechanisms for light emission in complexes with extended ligands.

The absorption spectra of $[\text{Ru}(\text{tpphz})(\text{phen})_2]^{2+}$ and $[\text{Ru}(\text{phehat})(\text{phen})_2]^{2+}$ display common features (Figure 4 and Table 3): (i) The first optical transition, 1, corresponds to a charge-transfer excitation to the π -extended ligand, at 2.79 eV in tpphz and 2.84 eV in phehat [to be compared with experimental values of 2.79 and 2.88 eV, respectively]; in both cases, the charge is transferred from the metal center to the phen sections of the

(82) Hay, P. J. *J. Phys. Chem. A* **2002**, *106*, 1634.

(83) Ghizdavu, L.; Lentzen, O.; Schumm, S.; Brodtkorb, A.; Moucheron, C.; Kirsch-De Mesmaeker, A. *Inorg. Chem.* **2003**, *42*, 1935.

(84) Pourtois, G.; Beljonne, D.; Moucheron, C.; Kirsch-De Mesmaeker, A.; Lazzaroni, R.; Brédas, J. L. Manuscript in preparation.

Table 3. Optically Allowed Electronic Transitions in $[\text{Ru}(\text{tpphz})(\text{phen})_2]^{2+}$ and $[\text{Ru}(\text{phehat})(\text{phen})_2]^{2+}$ Calculated at the INDO/SCI Level^a

$[\text{Ru}(\text{tpphz})(\text{phen})_2]^{2+}$				$[\text{Ru}(\text{phehat})(\text{phen})_2]^{2+}$			
<i>E</i> (eV)	OS	assignment		<i>E</i> (eV)	OS	assignment	
2.79 [2.79]	0.32	$\text{Ru} \rightarrow \pi^*_{\text{tpphz}}$	1	2.84 [2.88]	0.32	$\text{Ru} \rightarrow \pi^*_{\text{phehat}}$	1
3.26	0.14	$\text{Ru} \rightarrow \pi^*_{\text{phen}}$	2	3.21	0.13	$\text{Ru} \rightarrow \pi^*_{\text{phen}}$	2
3.31 [3.27]	0.46	$\pi_{\text{tpphz}} \rightarrow \pi^*_{\text{tpphz}}$		3.39 [3.34]	0.41	$\pi_{\text{phehat}} \rightarrow \pi^*_{\text{phehat}}$	
3.35	0.12	$\text{Ru} \rightarrow (\pi^*_{\text{phen}} + \pi^*_{\text{tpphz}})$		3.54	0.16	$\text{Ru} \rightarrow \pi^*_{\text{phehat}}$	
3.72 [3.46]	0.11	$\text{Ru} \rightarrow \pi^*_{\text{phen}}$	3	3.69	0.13	$\text{Ru} \rightarrow \pi^*_{\text{phen}}$	3
3.83 [3.95]	0.14	$\text{Ru} \rightarrow \pi^*_{\text{tpphz}}$		3.88	0.78	$\pi_{\text{phehat}} \rightarrow \pi^*_{\text{phehat}}$	
4.03 [3.98]	0.70	$\pi_{\text{tpphz}} \rightarrow \pi^*_{\text{tpphz}}$		4.09	0.32	$\pi_{\text{phehat}} \rightarrow \pi^*_{\text{phehat}}$	
4.03	0.12	$\text{Ru} \rightarrow \pi^*_{\text{phen}}$		4.29	0.45	$\pi_{\text{phehat}} \rightarrow \pi^*_{\text{phehat}}$	
4.28	0.21	$\pi_{\text{tpphz}} \rightarrow \pi^*_{\text{tpphz}}$		4.43	0.75	$\pi_{\text{phehat}} \rightarrow \pi^*_{\text{phehat}}$	4
4.35	0.22	$\pi_{\text{phen}} \rightarrow \pi^*_{\text{phen}}$	4	4.47	0.12	$\pi_{\text{phehat}} \rightarrow \pi^*_{\text{phehat}}$	
4.38	0.29	$\pi_{\text{phen}} \rightarrow \pi^*_{\text{phen}}$		4.51 [4.70]	0.68	$\pi_{\text{phehat}} \rightarrow \pi^*_{\text{phehat}}$	
4.45	0.11	$\text{Ru} \rightarrow \pi^*_{\text{tpphz}}$		4.69	0.15	$\text{Ru} \rightarrow \pi^*_{\text{phehat}}$	
4.50 [4.45]	0.63	$\pi_{\text{tpphz}} \rightarrow \pi^*_{\text{tpphz}}$		4.70	0.12	$\text{Ru} \rightarrow \pi^*_{\text{phehat}}$	
4.50	0.56	$\pi_{\text{tpphz}} \rightarrow \pi^*_{\text{tpphz}}$		4.90	0.33	$\text{Ru} \rightarrow \pi^*_{\text{phen}}$	5
4.74 [4.68]	0.29	$\text{Ru} \rightarrow \pi^*_{\text{tpphz}}$	5	4.99	0.95	$\pi_{\text{phen}} \rightarrow \pi^*_{\text{phen}}$	
4.82	0.19	$\pi_{\text{phen}} \rightarrow \pi^*_{\text{tpphz}}$		5.02	0.17	$\text{Ru} \rightarrow (\pi^*_{\text{phehat}} + \pi^*_{\text{phen}})$	
4.85	0.33	$\text{Ru} \rightarrow \pi^*_{\text{phen}}$		5.03	0.12	$(\text{Ru} + \pi_{\text{phehat}}) \rightarrow \pi^*_{\text{phehat}}$	
4.87	0.15	$\pi_{\text{phen}} \rightarrow \pi^*_{\text{tpphz}}$					
4.93	0.22	$\text{Ru} \rightarrow \pi^*_{\text{phen}} + \pi_{\text{phen}} \rightarrow \pi^*_{\text{phen}}$					
4.95	0.14	$\text{Ru} \rightarrow \pi^*_{\text{phen}} + \pi_{\text{phen}} \rightarrow \pi^*_{\text{phen}}$					
5.06	0.52	$\text{Ru} \rightarrow \pi^*_{\text{phen}} + \pi_{\text{phen}} \rightarrow \pi^*_{\text{phen}}$					

^a Only those excited states with calculated oscillator strengths ≥ 0.1 are included. *E* is the vertical transition energy and OS the associated oscillator strength. Experimental absorption maxima in acetonitrile are indicated within brackets.^{28,29,88}

extended ligands. (ii) $\pi-\pi^*$ excitations localized on the tpphz and phehat ligands (see bands 2–4, Figure 4) appear in the range 3.3–4.5 eV. (iii) Absorption by the phen moiety (band 5) occurs at higher energy (around 5.0 eV).

The predicted absorption spectra are in overall reasonable agreement with experiment, attesting the adequacy of the theoretical methodology for the description of the electronic structure and optical response of Ru complexes. We list in Tables 2 and 3 the energetic positions of the main absorption bands, as measured in acetonitrile solutions. In most ruthenium(II) complexes investigated, the computed energies of the $\text{MLCT}_{\text{phen}}$ and $\pi-\pi^*_{\text{phen}}$ transitions are overestimated by about 0.1–0.3 eV with respect to the experimental values. They are, however, slightly underestimated (by ~ 0.1 eV) when the dppz and phehat ligands are involved. A more detailed comparison between theory and experiment is presented elsewhere.⁸⁴

IV.2. Emission Properties. IV.2.a. Symmetric Complexes.

In the case of $[\text{Ru}(\text{bpy})_3]^{2+}$, it has been shown^{77–81} that optical absorption in the visible region populates the singlet metal-to-ligand charge-transfer (¹MLCT) excited states, which rapidly deactivate by intersystem crossing (within less than 1 ps)⁷⁹ to the lowest-lying MLCT triplet excited states (denoted ³MLCT). These ³MLCT excited states include three nearly degenerate triplet states (within a few inverse centimeters) as well as a fourth one, slightly higher in energy (by about 0.05 and 0.13 eV).⁷⁸ Thus, at room temperature, emission can, in principle, occur from a manifold of closely lying triplet states. Decay back to the ground state has been observed to occur via three different channels: (i) a radiative emission at 2.01 eV (in acetonitrile), (ii) a radiationless process, or (iii) a conversion to an upper metal-centered triplet excited state (³M) by thermal activation of the ³MLCT states. The efficiency of the latter depends on the energy separation (ranging from 0.31 to 0.56 eV, according to the ligand field strength)^{85,86} between the ³MLCT and ³M states.

The $[\text{Ru}(\text{bpy})_3]^{2+}$ complex is thus a candidate of choice to ascertain the reliability of our quantum-chemical approach. The description of the $[\text{Ru}(\text{bpy})_3]^{2+}$ excited states, as provided by the INDO/SCI method (Table 4), is in agreement with the experimental data: (i) A set of three nearly degenerate triplet ³MLCT states (T_1 , T_2 , T_3) is predicted at 2.42 eV. Note that T_2 and T_3 are the two components of a doubly degenerate *E'*-symmetry excited state. T_1 is an *A'*-symmetry excited state that is extremely close in energy to T_2 and T_3 as a result of the weak coupling of the excitations over the three ligands; see below.⁸⁷ (ii) A fourth state (T_4) is found at 2.66 eV. T_4 is nearly degenerate with two other triplet ³MLCT states (T_5 and T_6) (these, however, have not been identified experimentally). (iii) Degenerate metal-centered (³M) triplets (T_7 and T_8) are calculated at 3.25 eV, a finding that is consistent with the spectroscopic detection of a ³M state lying from 0.31 to 0.56 eV above the ³MLCT state manifold. The spin density distributions in the $[\text{Ru}(\text{bpy})_3]^{2+}$ triplet states (similar results are obtained for $[\text{Ru}(\text{phen})_3]^{2+}$) indicate a complete delocalization over the three ligands.

We have considered the two modes of relaxation described in the methodology section to model the geometric relaxation in the lowest triplet excited state of $[\text{Ru}(\text{bpy})_3]^{2+}$. As expected, when the geometry of a single unit is relaxed ($E^{\text{rel}} > V$), the degeneracy among the lowest excited states is lifted and the T_1 state is stabilized by about 0.6 eV (from 2.42 eV in the ground-state geometry to 1.85 eV in the excited-state geometry), whereas T_2 and T_3 remain quasi-degenerate (at 2.45 and 2.47 eV) as for the ground-state geometry. Delocalization of the geometric distortions over the three ligands ($V > E^{\text{rel}}$) leads to a stabilization by about 0.1 eV of all T_1 , T_2 , and T_3 excited states (from 2.42 eV in the ground-state geometry to ~ 2.30 eV in the excited-state geometry). In both scenarios (corresponding to weak and strong coupling), the computed energies are actually

(85) Meyer, T. J. *Pure Appl. Chem.* **1990**, *62*, 1003–1009.

(86) Van Houten, J.; Watts, R. J. *J. Am. Chem. Soc.* **1976**, *98*, 4853–4858.

(87) Beljonne, D.; Wenseleers, W.; Zojer, E.; Shuai, Z.; Vogel, H.; Pond, S. J. K.; Perry, J. W.; Marder, S. R.; Brédas, J. L. *Adv. Funct. Mater.* **2002**, *12*, 631.

Table 4. INDO/SCI Vertical Gas-Phase Energies of the Ten Lowest Lying Triplet States for $[\text{Ru}(\text{bpy})_3]^{2+}$, $[\text{Ru}(\text{phen})_3]^{2+}$, $[\text{Ru}(\text{dppz})(\text{phen})_2]^{2+}$, $[\text{Ru}(\text{tpphz})(\text{phen})_2]^{2+}$, and $[\text{Ru}(\text{phehat})(\text{phen})_2]^{2+}$ ^a

$[\text{Ru}(\text{bpy})_3]^{2+}$				$[\text{Ru}(\text{phen})_3]^{2+}$			
	<i>E</i> (eV)	sym	nature		<i>E</i> (eV)	sym	nature
T ₁	2.42	A'	³ MLCT	T ₁	2.29	A'	³ MLCT
T ₂ = T ₃	2.42	E'	³ MLCT	T ₂ = T ₃	2.29	E'	³ MLCT
T ₄	2.66	A'	³ MLCT	T ₄	2.55	A'	³ MLCT
T ₅ = T ₆	2.70	E'	³ MLCT	T ₅ = T ₆	2.57	E'	³ MLCT
T ₇ = T ₈	3.25	E'	³ M	T ₇ = T ₈	3.05	E'	³ MLCT
T ₉	3.33	A'	³ M	T ₉	3.05	A'	³ MLCT
T ₁₀	3.33	A'	³ M	T ₁₀	3.10	A'	³ M

$[\text{Ru}(\text{dppz})(\text{phen})_2]^{2+}$			$[\text{Ru}(\text{tpphz})(\text{phen})_2]^{2+}$			$[\text{Ru}(\text{phehat})(\text{phen})_2]^{2+}$		
	<i>E</i> (eV)	nature		<i>E</i> (eV)	nature		<i>E</i> (eV)	nature
T ₁	2.06 (2.08)	³ L _{dppz}	T ₁	2.26	³ L _{tpphz}	T ₁	2.36	³ L _{phehat}
T ₂	2.36 (2.44)	³ MLCT _{phen}	T ₂	2.40	³ L _{tpphz}	T ₂	2.42	³ MLCT _{phen}
T ₃	2.36 (2.46)	³ MLCT _{phen}	T ₃	2.42	³ MLCT _{phen}	T ₃	2.42	³ MLCT _{phen}
T ₄	2.42	³ L _{dppz}	T ₄	2.42	³ MLCT _{phen}	T ₄	2.44	³ L _{phehat}
T ₅	2.55	³ MLCT _{dppz}	T ₅	2.63	³ MLCT _{phen}	T ₅	2.64	³ MLCT _{phen}
T ₆	2.60	³ MLCT _{phen}	T ₆	2.66	³ MLCT _{tpphz}	T ₆	2.66	³ MLCT _{phehat}
T ₇	2.62	³ MLCT _{phen}	T ₇	2.66	³ MLCT _{phen}	T ₇	2.66	³ MLCT _{phen}
T ₈	2.67	³ MLCT _{dppz}	T ₈	2.78	³ MLCT _{tpphz}	T ₈	2.70	³ MLCT _{phehat}
T ₉	2.85	³ L _{dppz}	T ₉	3.00	³ L _{tpphz}	T ₉	2.97	³ L _{phehat}
T ₁₀	3.06	(³ LC + ³ MLCT) _{phen}	T ₁₀	3.07	³ MLCT _{phen}	T ₁₀	2.98	³ L _{phehat}

^a ³MLCT, ³M, and ³L correspond to a metal-to-ligand charge transfer, a metal-centered triplet state, and a ligand-centered triplet state, respectively. The TDDFT gas-phase energies for $[\text{Ru}(\text{dppz})(\text{phen})_2]^{2+}$ are indicated in parentheses.

within a few tenths of an electronvolt of the measured emission peaking at 2.01 eV in acetonitrile.^{77–81}

To determine the most likely scenario, we can try to estimate the relative amplitude of the relaxation energy (E^{rel}) and the electronic coupling among the ligands (V). In C_3 -symmetry compounds, the electronic coupling among ligands is related to the energy difference between the adiabatic A' and E' triplet excited states in the ground-state geometry:⁸⁷ $V = (E_{T_2} - E_{T_1})/3$. The relative orientations of the ligands in $[\text{Ru}(\text{bpy})_3]^{2+}$ lead to a very weak coupling ($V \approx 0.004$ eV). On the other hand, the relaxation energy in an isolated ligand is estimated to be about 0.6 eV. Since $E^{\text{rel}} \gg V$, the excitation localization scenario is expected to be more relevant than excitation delocalization, which seems to be consistent with the observations by Yeh et al.⁷⁵ However, as pointed out above, excitation localization implies that the triplet excited states do not remain degenerate and a gap of at least a few tenths of an electronvolt should open up between T₁ and T₂; to the best of our knowledge, this has not been observed by Yeh et al.⁷⁵ On the other hand, the excitation delocalization scheme preserves the triplet-state degeneracy and seems to provide a representation of the lowest lying triplet excited states that is more consistent with classical views.^{77–81} The current work does not allow ruling out any of these two limiting cases (it is possible that at early times a coherent superposition of excitations over the three branches is formed, which then relaxes into a localized excitation over a single arm as a result of coupling to vibrations, conformational changes, or any source of disorder or fluctuation due to the environment).

The description of the triplet-state properties for $[\text{Ru}(\text{phen})_3]^{2+}$ is similar to that of $[\text{Ru}(\text{bpy})_3]^{2+}$ (Table 4): (i) the three lowest triplet states (T₁, T₂, T₃) are degenerate (at 2.29 eV) and correspond to ³MLCT states; (ii) there are two sets of triplet ³MLCT states at 2.55–2.57 (T₄, T₅, T₆) and 3.05 eV (T₇, T₈, T₉), followed by (iii) a metal-centered (³M) triplet at 3.10 eV. As in the case of $[\text{Ru}(\text{bpy})_3]^{2+}$, the excited-state relaxation phenomena have been modeled by considering both delocalized

and localized limits. For the weak coupling scenario, the relaxation of a phen unit breaks the molecular D_3 symmetry and stabilizes T₁ at 1.83 eV; in the case of full delocalization, the geometric deformations spread over the three phen units and shift the energy of T₁, T₂, and T₃ by 0.22 eV, from 2.29 to 2.07 eV. As in $[\text{Ru}(\text{bpy})_3]^{2+}$, the computed energies for the two extreme cases of lattice relaxation “bracket” the experimental value² (2.08 eV), which does not allow us to draw any definitive conclusion. The same considerations as for $[\text{Ru}(\text{bpy})_3]^{2+}$ suggest that $[\text{Ru}(\text{phen})_3]^{2+}$ belongs to the weak coupling regime ($V \ll E^{\text{rel}}$); thus, the initially delocalized excited state is expected to be unstable with respect to geometric distortions, leading to (at least partial) localization of the excitation on a single ligand.

IV.2.b. Complexes with an Extended Ligand. The photoluminescence quantum yield^{28,29,88,89} in $[\text{Ru}(\text{dppz})(\text{phen})_2]^{2+}$, $[\text{Ru}(\text{tpphz})(\text{phen})_2]^{2+}$, and $[\text{Ru}(\text{phehat})(\text{phen})_2]^{2+}$ is extraordinarily sensitive to the nature of the surrounding medium. The emission yield has been reported to be vanishingly small in water, but weak to moderate in nonaqueous media such as ethanol and acetonitrile, respectively. Interestingly, luminescence increases tremendously when the complex is intercalated in DNA; such a phenomenon has been denoted as a “light-switch” effect.²³ The origin of this emission sensitivity to the medium is related to the nature of the triplet states involved in the emission process. Olson et al.³⁰ demonstrated, on the basis of time-correlated single photon counting measurements, that the quasi-negligible emission of $[\text{Ru}(\text{dppz})(\text{phen})_2]^{2+}$ in water arises from a presumed ³MLCT state located at 1.56 eV, characterized by a rapid radiationless decay ($\tau = 250$ ps) as also measured by Önfelt et al.,⁹⁰ and a low emission quantum yield ($\phi_{\text{lum}} = 2.5 \times 10^{-6}$). They also observed that the emission shifts from a low-lying short-lived species at 1.56 eV in water or in an acetonitrile/water mixture to a longer lived excited species (τ

(88) Campagna, S.; Serroni, S.; Bodige, S.; MacDonnell, F. M. *Inorg. Chem.* **1999**, *38*, 692.

(89) Nair, R. B.; Cullum, B. M.; Murphy, C. J. *Inorg. Chem.* **1997**, *36*, 926.

(90) Önfelt, B.; Lincoln, P.; Nordén, B.; Baskin, J. S.; Zewail, A. H. *Proc. Natl. Acad. Sci. U.S.A.* **2000**, *97*, 5708.

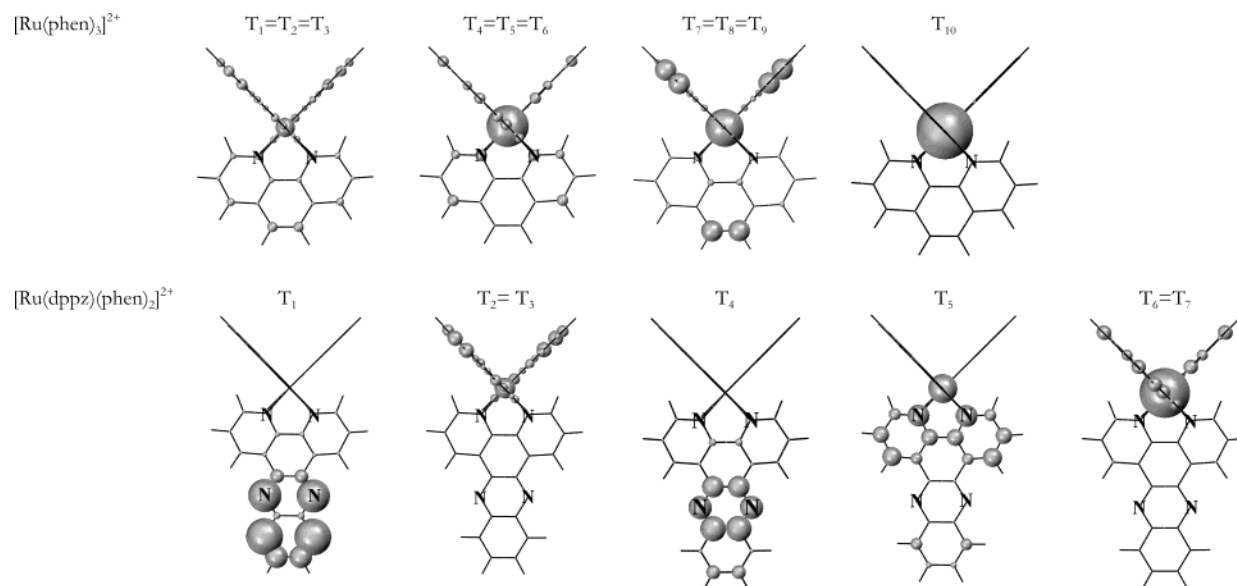


Figure 5. INDO/SCI spin density distributions computed in the lowest lying triplet states of $[\text{Ru}(\text{phen})_3]^{2+}$ and $[\text{Ru}(\text{dppz})(\text{phen})_2]^{2+}$. As for the symmetric complexes, the explicit relaxation of the triplet states on either dppz or the phen section of $[\text{Ru}(\text{dppz})(\text{phen})_2]^{2+}$ has been taken into account. The introduction of the relaxed triplet geometry of dppz in $[\text{Ru}(\text{dppz})(\text{phen})_2]^{2+}$ stabilizes T_1 (${}^3\text{L}_{\text{dppz}}$) from 2.06 to 1.65 eV.

= 660 ns) at 1.97 eV in pure acetonitrile, characterized by a larger quantum yield ($\phi_{\text{lum}} = 3.3 \times 10^{-2}$). More recently, Coates et al.⁹¹ have reported the differential absorption of the 250 ps transient in water (peaking at ~ 550 nm). This species has been attributed to a ${}^3\text{MLCT}$ dppz stabilized by H-bonding.^{30,90} H-bonding formation has also been elegantly demonstrated from kinetic treatments of luminescence data in glycerol.³¹ On the other hand, the presence of another low-lying excited state *in aprotic solvents* was inferred by Brennaman et al.,³² to explain the abnormal temperature dependence of emission lifetime in $[\text{Ru}(\text{dppz})(\text{bpy})_2]^{2+}$, where a maximum of lifetime was measured in the low-temperature region. The authors concluded the existence of an equilibrium between a low-lying dark state and a luminescent state, both of ${}^3\text{MLCT}$ type, entropically driven toward the bright state at room temperature.

The INDO/SCI calculations indicate that, in contrast to $[\text{Ru}(\text{phen})_3]^{2+}$ and $[\text{Ru}(\text{bpy})_3]^{2+}$, $[\text{Ru}(\text{dppz})(\text{phen})_2]^{2+}$ has a T_1 state, at 2.06 eV, that is completely localized on dppz (${}^3\text{L}$). The spin density distribution is actually very similar to that of the free ligand; see Figures 3 and 5. T_2 , T_3 , and T_5 (at 2.36 and 2.55 eV, respectively) correspond to more conventional ${}^3\text{MLCT}$ states involving either the phen or dppz ligand (see $[\text{Ru}(\text{phen})_3]^{2+}$ and $[\text{Ru}(\text{dppz})(\text{phen})_2]^{2+}$, Figure 5 and Table 4). Note that (i) this description is fully supported by the results of the TDDFT calculations, which provide not only a similar ordering of the lowest excited states but also excitation energies very close to the INDO/SCI values (see Table 4), and (ii) the spin density distribution of T_4 is similar to that of T_2 in free dppz. Relaxing the triplet state on one phen unit induces a stabilization of the ${}^3\text{MLCT}_{\text{phen}}$ localized triplet by 0.49 eV from 2.36 to 1.87 eV, which is in good agreement with the experimental measurement of the $[\text{Ru}(\text{dppz})(\text{phen})_2]^{2+}$ emission in acetonitrile at 1.97 eV.

It is generally accepted that the presence of heavy atoms (such as ruthenium) induces some localization of the triplet state on the metal core and enhances the spin–orbit coupling. On that

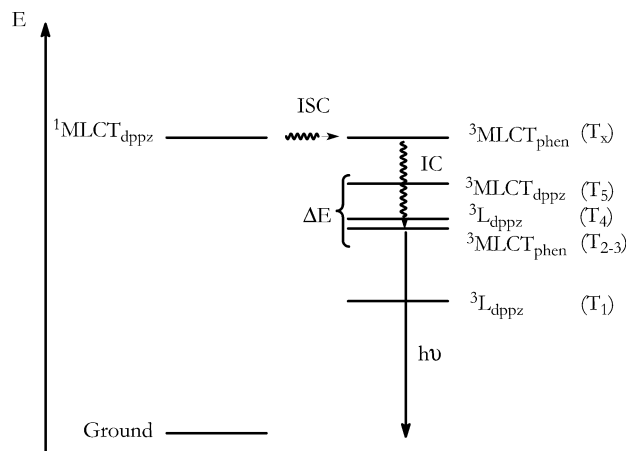


Figure 6. Schematic representation of the excited states proposed for the emission process taking place in $[\text{Ru}(\text{dppz})(\text{phen})_2]^{2+}$ in acetonitrile.

basis, one can argue that the absence of a sizable ruthenium contribution on T_1 should be associated with a weak spin–orbit coupling and disfavor the radiative process. The situation is very different for the higher lying triplet states (T_2 and T_3), where the spin density is delocalized over the ruthenium and the ligands. This is expected to enhance the spin–orbit coupling and hence should lead to more efficient decay from these states back to the ground state. In Figure 6, a schematic energy diagram including the relevant excited states, as calculated at the INDO level, is shown for the $[\text{Ru}(\text{dppz})(\text{phen})_2]^{2+}$ complex.

We now discuss how recent experimental investigations on the rich photophysics of Ru complexes including extended ligands can be interpreted on the basis of our theoretical results. The calculated energy difference between the higher ${}^3\text{MLCT}$ excited states is rather small (close to 0.2 eV; see ΔE in Figure 6). Moreover, the difference between these states and the lowest lying T_1 (${}^3\text{L}$) state could be reduced when solvent effects are accounted for in the triplet states (since, by definition, MLCT states possess larger state dipoles than LC states). On that basis, and keeping in mind the model proposed by Brennaman et al.³² to explain the temperature-dependent emission lifetime of $[\text{Ru}$

(91) Coates, C. G.; Olofsson, J.; Coletti, M.; McGravey, J. J.; Önfelt, B.; Lincoln, P.; Nordén, B.; Tuite, E.; Matousek, P.; Parker, A. W. *J. Phys. Chem. B* **2001**, *105*, 12653.

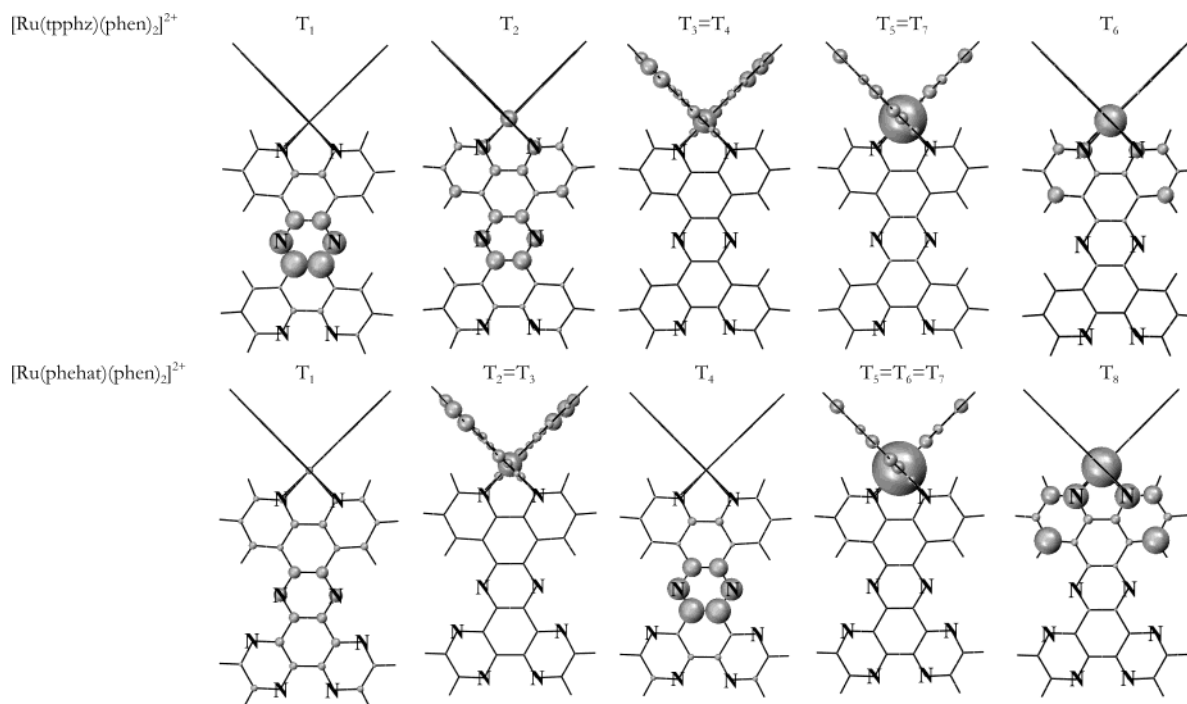


Figure 7. INDO/SCI spin density distributions computed for the lowest lying triplet states in the $[\text{Ru}(\text{tpphz})(\text{phen})_2]^{2+}$ and $[\text{Ru}(\text{phehat})(\text{phen})_2]^{2+}$ complexes.

$(\text{dppz})(\text{bpy})_2]^{2+}$ in aprotic solvents, we propose that the T_1 (${}^3L_{\text{dppz}}$) excited state actually plays the role of the low-lying “dark” state of ref 32 and is characterized by a nonradiative decay rate constant of the same order as the deactivation rate constant of ${}^3\text{MLCT}$ states. Thus, according to the present calculations, the lowest calculated ${}^3\text{MLCT}$ excited state in MeCN and other aprotic solvents (characterized by a larger singlet–triplet mixing) would be in equilibrium with the lower lying T_1 ${}^3L_{\text{dppz}}$ dark state. Since radiative decay from T_1 is slow, the deactivation paths from the ligand-centered excited state should be mostly nonradiative.

According to this scenario, the emission properties when the temperature is decreased would result from the tradeoff between two competing processes: crossing to the higher ${}^3\text{MC}$ state, which would result in increased lifetimes, and a shift of the equilibrium to and decay from the lower ${}^3\text{LC}$, leading to decreased lifetimes. Depending on the temperature and the resulting relative magnitude of the involved kinetic constants, a maximum in the measured luminescence lifetimes is expected and has indeed been reported in ref 32. At very low temperature, however, in a frozen matrix at 77 K, a structured emission signal associated with the lowest lying ${}^3L_{\text{dppz}}$ excited state might be expected, which so far has not been observed experimentally. It has to be mentioned that the $\text{Re}(\text{I})\text{--dppz}$ ⁹² or $\text{Rh}(\text{III})$ complexes⁸³ exhibit both types of luminescence at 77 K.

To account for the complicated photophysics of these complexes in water requires to explicitly account for the presence of the solvent, which is a formidable task from a theoretical point of view and has not been achieved here (attempts to describe the effects of hydrogen bonds on the excited-state description of $[\text{Ru}(\text{dppz})(\text{phen})_2]^{2+}$ were not conclusive). It is entirely conceivable that the ${}^3\text{MLCT}_{\text{dppz}}$ excited state stabilized in hydroxylated solvents produces H-bonded

excited species of much lower energy that could act as emission centers, as has been proposed by several groups.^{30,31} We stress that such a species could not correspond to T_1 , although the energy of the relaxed T_1 ${}^3L_{\text{dppz}}$ excited state is close to that of the emission detected in water, as the 250 ps T–T transient absorption shows a maximum at ~ 550 nm,⁹¹ which is significantly off the position of the T–T absorption peak of the ${}^3L_{\text{dppz}}$ in $\text{Re}(\text{I})$ (peaking around 460 nm). In addition, such a low-energy emission in hydroxylated solvent, if corresponding to T_1 , would also be observed in acetonitrile, unless invoking exceedingly slow (microseconds) internal conversion from ${}^3\text{MLCT}$ (T_2 , T_3) to ${}^3\text{LC}$ (T_1) excited states. We therefore conclude that the dark state observed by Brennaman et al. and the short-lived excited state responsible for emission in water are two distinct excited states. While the first one could be assigned as the ${}^3L_{\text{dppz}}$ excited state, the second one most likely arises from specific interactions between the complex and the solvent in a ${}^3\text{MLCT}$ -type excited species.

The descriptions of the $[\text{Ru}(\text{tpphz})(\text{phen})_2]^{2+}$ and $[\text{Ru}(\text{phehat})(\text{phen})_2]^{2+}$ triplet states present features common to $[\text{Ru}(\text{dppz})(\text{phen})_2]^{2+}$: the T_1 state of both complexes is localized on the π -extended ligand and closely resembles T_1 of the isolated ligands (the spin density is confined on the central pyrazine core for tpphz and is delocalized over the ligand for phehat ; see Figures 3 and 7). At higher energies, the triplets form three bands of closely lying excited states at ~ 2.40 eV (T_2 , T_3 , T_4), 2.60 eV (T_5 , T_6 , T_7), and 3.00 eV (T_8 , T_9 , T_{10}). This triplet manifold is constituted of (i) charge-transfer excited states, involving either phen (T_3 , T_4 , T_5 , T_7 and T_{10} for $[\text{Ru}(\text{tpphz})(\text{phen})_2]^{2+}$ and T_2 , T_3 , T_5 and T_7 for $[\text{Ru}(\text{phehat})(\text{phen})_2]^{2+}$) or $\text{tpphz}/\text{phehat}$ (T_6 and T_8 for $[\text{Ru}(\text{tpphz})(\text{phen})_2]^{2+}$ and $[\text{Ru}(\text{phehat})(\text{phen})_2]^{2+}$) and (ii) ligand-localized triplet states (T_2 and T_9 for $[\text{Ru}(\text{tpphz})(\text{phen})_2]^{2+}$ and T_4 , T_9 and T_{10} for $[\text{Ru}(\text{phehat})(\text{phen})_2]^{2+}$).

(92) Stoeffler, H. D.; Thornton, N. B.; Temkin, S. L.; Schanze, K. S. *J. Am. Chem. Soc.* **1995**, *117*, 7119.

As for $[\text{Ru}(\text{dppz})(\text{phen})_2]^{2+}$, the emission of $[\text{Ru}(\text{tpphz})(\text{phen})_2]^{2+}$ or $[\text{Ru}(\text{phehat})(\text{phen})_2]^{2+}$ is quasi-negligible in the presence of water.^{20,27,28} These complexes might exhibit an emission lifetime behavior in aprotic solvents similar to that of $[\text{Ru}(\text{phen})_2(\text{dppz})]^{2+}$ so that they would probably belong to the same family of compounds. Concerning the theoretical calculations, note that relaxation of the triplet state on a phen unit stabilizes the ${}^3\text{MLCT}_{\text{phen}}$ state for $[\text{Ru}(\text{tpphz})(\text{phen})_2]^{2+}$ and $[\text{Ru}(\text{phehat})(\text{phen})_2]^{2+}$ at around 1.83 eV; this value is very close to that calculated for the relaxed triplet excited state localized on either tpphz (1.80 eV) or phehat (1.90 eV). Therefore, the energy difference between the ${}^3\text{MLCT}_{\text{phen}}$ and ${}^3\text{L}_{\text{phehat/tpphz}}$ excited states is too small (0.03–0.07 eV) in this case to allow the contributions from the two channels to be distinguished on the basis of the calculations. Experimentally, $[\text{Ru}(\text{tpphz})(\text{phen})_2]^{2+}$ and $[\text{Ru}(\text{phehat})(\text{phen})_2]^{2+}$ ${}^3\text{MLCT}$ emissions are observed in acetonitrile at 1.98 eV⁸⁸ and 1.90 eV,²⁸ respectively.

V. Conclusions

We have used a theoretical approach based on correlated quantum-chemical calculations to describe the singlet and excited states in a series of polyazaaromatic ruthenium(II) complexes and their associated free ligands. Our quantum-chemical analysis provides a detailed insight into the nature and the localization of the singlet and triplet states that are relevant for the optical absorption and emission properties of these complexes.

In the compounds we investigated, the emission process comes from a manifold of triplet states, the composition of which depends on the nature of the ligands. In complexes where the ligands contain a relatively confined aromatic backbone, such as phen or bpy, the lowest lying triplet states are ${}^3\text{MLCT}$ -

like excited states and light emission is relatively insensitive to the presence of water. Moreover, the emission lifetime as a function of temperature has a normal behavior. In contrast, the emission of complexes containing π -extended ligands, such as dppz, tpphz, and phehat, is extremely sensitive to the surrounding medium, and the luminescence lifetime shows an abnormal dependence on temperature in aprotic solvents (at least for the related complex $[\text{Ru}(\text{dppz})(\text{bpy})_2]^{2+}$ ³²). We propose to associate this abnormal behavior with the presence of a low-lying triplet state centered mainly on the pyrazine section of the π -extended ligand, called the dark state in a previously proposed model.³² Ru contribution to the wave function in this ligand-centered excited state is weak, leading to a low radiative decay, which could be responsible for this effect. The present study does not, however, provide a clue as to the origin of the emission in water; work is now in progress to investigate this point further.

Acknowledgment. The work at The University of Arizona is supported by the National Science Foundation (Grant CHE-0078819), the Office of Petroleum Research Fund, and the IBM Shared University Research Program. The work at the University of Mons-Hainaut is supported by the Belgian Federal Government “InterUniversity Attraction Pole in Supramolecular Chemistry and Catalysis (PAI 5/3)” and the Belgian National Fund for Scientific Research (FNRS-FRFC). D.B. is Senior FNRS Research Associate and R.L. is FNRS Research Director. S.S. thanks the European TMR program (Grant ERBFM-RXCT 980226) for a fellowship. C.M. and A.K.D. are grateful to the ARC program of the “Communauté Wallonie-Bruxelles” for financial support.

JA034444H